Electron-hole pair condensation at the semimetal-semiconductor transition: A BCS-BEC crossover scenario

B. Zenker,[1] D. Ihle,[2] F. X. Bronold,[1] and H. Fehske[1]

[1]*Institut für Physik, Ernst-Moritz-Arndt-Universität Greifswald, D-17487 Greifswald, Germany*
[2]*Institut für Theoretische Physik, Universität Leipzig, D-04109 Leipzig, Germany*

We act on the suggestion that an excitonic insulator state might separate—at very low temperatures—a semimetal from a semiconductor and ask for the nature of these transitions. Based on the analysis of electron-hole pairing in the extended Falicov-Kimball model, we show that tuning the Coulomb attraction between both species, a continuous crossover between a BCS-like transition of Cooper-type pairs and a Bose-Einstein condensation of preformed tightly bound excitons might be achieved in a solid-state system. The precursor of this crossover in the normal state might cause the transport anomalies observed in several strongly correlated mixed-valence compounds.

The challenging suggestion of electron-hole pair condensation in thermal equilibrium into the excitonic insulator (EI) phase at the semimetal (SM) to semiconductor (SC) transition,[1] where the SM-EI transition may be described in analogy with BCS theory of superconductivity and the SC-EI transition is discussed in terms of a Bose-Einstein condensation (BEC) of preformed excitons,[2–4] is of topical interest. This is due to the growing amount of experimental data on materials which are candidates for the realization of the EI, where different situations with respect to the SM/SC-EI transition are given. For example, in the rare-earth chalcogenide $TmSe_{0.45}Te_{0.55}$, that is, an intermediate-valent SC, the pressure-induced resistivity anomaly at low temperatures was ascribed to exciton formation and a subsequent SC-EI transition.[5–8] An EI state in semiconducting Ta_2NiSe_5 was recently probed by photoemission.[9] On the other hand, in the layered transition-metal dichalcogenide $1T$-$TiSe_2$, which is a SM, a BCS-like electron-hole pairing was considered as the driving force for the periodic lattice distortion.[10] Here evidence suggests electron-hole "Cooper-pair" fluctuations above the SM-EI transition temperature. A BCS-like electron-hole pair condensation was also studied for graphene bilayers.[11] In this system a BCS-BEC crossover might be realized by a magnetic field that creates a gap and magnetoexcitons which may condense. From a theoretical point of view, one of the main issues in this field is the better understanding and a detailed description of the normal phase above the SM/SC-EI transition, especially of the electron-hole pair fluctuations and of the BCS-BEC crossover scenario[12] that characterizes the EI instability and, to the best of our knowledge, has not been observed in a solid so far.

In this Rapid Communication we address this topic and the mechanisms behind in terms of a minimal two-band model, the so-called extended Falicov-Kimball model (EFKM),[3,13,14] which covers direct c- and f-band hopping and admits the pairing of c electrons with f holes via a strongly screened Coulomb interaction. Thereby we focus on the normal phase that surrounds the EI and look for precursor effects in the electron-hole pair susceptibility. In particular, we analyze the nature of the electron-hole bound states and determine their number and spectral weight. We are able to show how the

normal state to EI transition changes from BCS to BEC when the SM gives way to the SC.

Representing the orbital flavor of the f,c electrons by the pseudospin $\sigma = \uparrow, \downarrow$, the EFKM takes the form

$$H = \sum_{\mathbf{k},\sigma} \varepsilon_{\mathbf{k}\sigma} n_{\mathbf{k}\sigma} + U \sum_i n_{i\uparrow} n_{i\downarrow}. \quad (1)$$

Equation (1) constitutes a generalized Hubbard model with on-site Coulomb interaction U and spin-dependent band energies $\varepsilon_{\mathbf{k}\sigma} = E_\sigma - t_\sigma \gamma_{\mathbf{k}} - \mu$, where E_σ defines the band center of the σ band, t_σ denotes the nearest-neighbor hopping amplitude on a D-dimensional hypercubic lattice, $\gamma_{\mathbf{k}} = 2 \sum_{d=1}^D \cos k_d$, and μ is the chemical potential. For $E_\uparrow < E_\downarrow$ and $t_\uparrow t_\downarrow < 0$ ($t_\uparrow t_\downarrow > 0$) a direct (indirect) band gap might appear. The σ-electron density is given by $n_\sigma = \frac{1}{N} \sum_{\mathbf{k}} \langle n_{\mathbf{k}\sigma} \rangle = \frac{1}{N} \sum_{\mathbf{k}} \langle c_{\mathbf{k}\sigma}^\dagger c_{\mathbf{k}\sigma} \rangle$, and we require $n_\uparrow + n_\downarrow = 1$ for the half-filled band case.

The EI low-temperature phase of the EFKM is characterized by a nonvanishing order parameter $\Delta = \frac{U}{N} \sum_{\mathbf{k}} \langle c_{\mathbf{k}\downarrow}^\dagger c_{\mathbf{k}\uparrow} \rangle$ (in case of a direct band gap).[3,14,15] Describing a condensate of electron-hole pairs (excitons), Δ obeys a gap equation with anomalous Green's functions involved.[2,4,10] From this the transition temperature $T_{EI}(U)$ can be determined. In what follows we scrutinize the existence of excitonic bound states above T_{EI} where $\Delta = 0$. To this end we analyze the susceptibility $\chi_{\mathbf{q}}^{\uparrow,\downarrow}(\omega) = \langle\langle b_{\mathbf{q}}; b_{\mathbf{q}}^\dagger \rangle\rangle_\omega$, with $b_{\mathbf{q}}^\dagger = \frac{1}{\sqrt{N}} \sum_{\mathbf{k}} c_{\mathbf{k}+\mathbf{q}\downarrow}^\dagger c_{\mathbf{k}\uparrow}$ creating an electron-hole excitation with momentum $\mathbf{q}$ in the SM and SC high-temperature phases. The pole of $\chi_{\mathbf{q}}^{-\sigma,\sigma}(\omega)$, $\omega_X(\mathbf{q}) = \omega_X^{\uparrow,\downarrow}(\mathbf{q}) = -\omega_X^{\downarrow,\uparrow}(\mathbf{q})$, calculated in ladder approximation, describes an exciton, provided that $0 < \omega_X(\mathbf{q}) < \omega_C(\mathbf{q})$. Here $\omega_C(\mathbf{q}) = \min_{\mathbf{k}}(\tilde{\varepsilon}_{\mathbf{k}+\mathbf{q}\downarrow} - \tilde{\varepsilon}_{\mathbf{k}\uparrow})$ is the lower bound of the electron-hole excitations and $\tilde{\varepsilon}_{\mathbf{k}\sigma}$ denotes the renormalized band structure. The binding energy of the exciton is $E_B^X(\mathbf{q}) = \omega_C(\mathbf{q}) - \omega_X(\mathbf{q})$. Outside the electron-hole continuum the imaginary part of $\chi_{\mathbf{q}}^{-\sigma,\sigma}$ is

$$\mathrm{Im}\chi_{\mathbf{q}}^{-\sigma,\sigma}(\omega) = -\pi \, Z(\omega_X,\mathbf{q})\,\delta\big(\omega - \omega_X^{-\sigma,\sigma}\big), \quad (2)$$

where

$$Z(\omega_X,\mathbf{q}) = \left[\frac{U^2}{N} \sum_{\mathbf{k}} \frac{f(\tilde{\varepsilon}_{\mathbf{k}\uparrow}) - f(\tilde{\varepsilon}_{\mathbf{k}+\mathbf{q}\downarrow})}{(\omega_X + \tilde{\varepsilon}_{\mathbf{k}\uparrow} - \tilde{\varepsilon}_{\mathbf{k}+\mathbf{q}\downarrow})^2}\right]^{-1} \quad (3)$$

gives the spectral weight of the excitonic quasiparticle.

To determine the chemical potential including self-energy effects, we expand the imaginary part of $G_{\mathbf{k}\sigma}(\omega) = [\omega - \bar{\varepsilon}_{\mathbf{k}\sigma} - \Sigma_{\mathbf{k}\sigma}(\omega)]^{-1}$, where $\bar{\varepsilon}_{\mathbf{k}\sigma} = \varepsilon_{\mathbf{k}\sigma} + U n_{-\sigma}$, for small damping. The self-energy is obtained by the Green's function projection technique[16]

$$\Sigma_{\mathbf{k}\sigma}(\omega) = -\frac{U^2}{N\pi^2} \sum_{\mathbf{k}'} \int d\bar{\omega} \int d\omega' \frac{[f(\omega') + p(\omega' - \bar{\omega})]}{\omega - \bar{\omega}}$$
$$\times \operatorname{Im}\chi_{\mathbf{k}-\mathbf{k}'}^{-\sigma,\sigma}(\bar{\omega} - \omega')\operatorname{Im}G_{\mathbf{k}'-\sigma}(\omega'), \qquad (4)$$

with $f(\omega) = [e^{\beta\omega} + 1]^{-1}$, $p(\omega) = [e^{\beta\omega} - 1]^{-1}$. Considering the parameter region near the SM/SC-EI transition, where the dominant weight of the electron-hole spectral function is suggested to arise from the bound state as compared with the electron-hole continuum, in the self-energy calculation we take into account only the excitonic quasiparticle contribution given by Eq. (2). Then the σ-electron density can be decomposed into a part of nearly-free electrons (with renormalized dispersion) and a term $\propto\operatorname{Im}\Sigma_{\mathbf{k}\sigma}(\omega)$ that comprises the electron-bound states as well as the reaction of the σ electrons to the existence of excitons. Denoting the latter contribution as the correlation part, we have $n_\sigma = n_\sigma^{\mathrm{nf}} + n_\sigma^{\mathrm{corr}}$, and find $n_\sigma^{\mathrm{nf}} = \frac{1}{N}\sum_{\mathbf{k}} f(\tilde{\varepsilon}_{\mathbf{k}\sigma})$, where $\tilde{\varepsilon}_{\mathbf{k}\sigma} = \bar{\varepsilon}_{\mathbf{k}\sigma} + \operatorname{Re}\Sigma_{\mathbf{k}\sigma}(\omega)|_{\omega=\tilde{\varepsilon}_{\mathbf{k}\sigma}}$. It turns out that $n_\uparrow^{\mathrm{corr}} = -n_\downarrow^{\mathrm{corr}}$. Hence, the chemical potential can be obtained by using solely the nearly-free part of the particle densities, i.e., $n_\uparrow + n_\downarrow = n_\uparrow^{\mathrm{nf}} + n_\downarrow^{\mathrm{nf}} = 1$ (cf. also Ref. [2]).

The number of excitons with center-of-mass momentum $\mathbf{q}$ results in

$$N_X(\mathbf{q}) = \langle b_{\mathbf{q}}^\dagger b_{\mathbf{q}}\rangle|_{\omega_X} = Z(\omega_X,\mathbf{q})p(\omega_X), \qquad (5)$$

leading to the total exciton density $n_X = \frac{1}{N}\sum_{\mathbf{q}} N_X(\mathbf{q})$. To characterize the composition of the normal phase, we introduce the bound-state fractions $\Gamma = n_X/(n_X + n_\downarrow^{\mathrm{nf}})$ and $\Gamma_0 = N_X(0)/N(n_X + n_\downarrow^{\mathrm{nf}})$.

To simplify the numerical analysis, we discard the band renormalization of the σ electrons by the excitons, i.e., we neglect the term $\propto\operatorname{Re}\Sigma$ in $\tilde{\varepsilon}_{\mathbf{k}\sigma}$. Then n_σ^{nf} contains the Hartree shift $U n_{-\sigma}$ only and, inserting the nearly-free part of $G_{\mathbf{k}\sigma}$ into $\Sigma_{\mathbf{k}\sigma}$ $\chi_{\mathbf{q}}^{-\sigma,\sigma}$ becomes the random phase approximation (RPA) result. Since the ground-state phase diagram of the EFKM is similar in two dimensions (2D) and three dimensions (3D),[13,14] and we are primary interested in the normal-state properties for $T > T_{\mathrm{EI}}$, we consider the 2D case hereafter. To model an intermediate-valence situation we choose $E_\uparrow = -2.4$, $E_\downarrow = 0$, $t_\uparrow = -0.8$ without loss of generality, and take $t_\downarrow = 1$ as energy unit.

The RPA EFKM phase diagram shown in Fig. 1 describes the general scenario at the SM-SC transition, which persists, apart from a reduction of the critical temperature, also when the electronic correlations are treated by the more elaborate slave boson approach.[15] The SM (SC) has a gapless (gapful) band structure with a small band overlap (band gap). The metal-insulator transition is triggered by enlarging the Hartree shift upon increasing U. The phase boundary to the EI can be obtained from a BCS-like gap equation, which holds on both SM and SC sides, but gives no detailed insight into the nature of this transition.

Now, let us take a closer look as to how the excitonic instability develops in the SM and SC regimes (cf. Figs. 1–3).
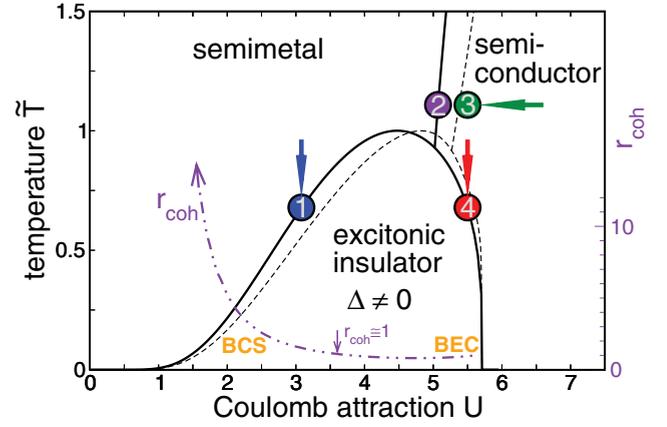

FIG. 1. (Color online) EI formation at the SM-SC transition in the 2D EFKM. The phase diagram is calculated for a band splitting $E_\uparrow - E_\downarrow = -2.4$, and band asymmetry $t_\uparrow/t_\downarrow = -0.8$, where the temperature T is scaled to the maximum critical temperature $\tilde{T} = T/T_{\mathrm{EI}}^{\mathrm{max}}$ with $T_{\mathrm{EI}}^{\mathrm{max}} = 0.361$ (RPA, solid line) and $T_{\mathrm{EI}}^{\mathrm{max}} = 0.256$ (slave boson, thin dashed line). The coherence length of the EI condensate at $\tilde{T} = 0$, r_{coh} (as defined in Ref. [4]), is indicated by the dotted-dotted-dashed line.

We start with the SM (point 1 in Fig. 1). Here the valence and conduction bands slightly overlap; as a result a distinct Fermi surface exists (see Fig. 2, blue frame). Approaching T_{EI}, the electron-hole pair fluctuations contained in $\chi_{\mathbf{q}}^{-\sigma,\sigma}$ become critical and will drive a phase transition, which is accompanied by a spontaneous hybridization of the $\uparrow$ and $\downarrow$ bands.[10] The resulting energy spectrum exhibits a gap at the Fermi level, where the density of states is largely enhanced at the top (bottom) of the lower (upper) quasiparticle band.[3,15] The pivotal question is whether excitons are involved in this BCS-like transition. While excitonic bound states might exist above T_{EI} (in the region given by the red line), we definitely have no excitons with $\mathbf{q} = 0$. In either case, $Z(\omega_X,\mathbf{q})$ is zero except near the corners of the Brillouin zone [see Fig. 3(b)], and the number of these excitons, having a large center-of-mass momentum, is very small [see $N_X(\mathbf{q})$ in Fig. 2]. Hence, the formation of the EI state in the SM region is barely influenced by excitons.

A larger Coulomb interaction U will affect the system in two ways: It (i) increases the bare band splitting and (ii) amplifies the attraction between electrons and holes. At the SM-SC transition (point 2 in Fig. 1, purple frame in Fig. 2), the $\uparrow$ and $\downarrow$ bands only touch each other (at $\mathbf{k} = 0$). Accordingly the Fermi surface shrinks in size to a point. In this case a larger number of excitons form (also with small momenta), but again the zero-momentum excitons play no significant role because of the conelike structure of $Z(\omega_X,\mathbf{q})$; see Fig. 3(c).

In the SC region (point 3 in Fig. 1, green frame in Fig. 2) the (Hartree) band structure exhibits a direct gap, within which the chemical potential μ and the exciton level ω_X are located. Now zero-momentum excitons may occur. Although having the lowest binding energy, they represent the largest contribution to the total number of excitons. Here $Z(\omega_X,\mathbf{q})$ is finite for all momenta. Actually the system now realizes a three-component plasma consisting of electrons, holes, and excitons. Lowering the temperature, the excitonic level moves toward the valence
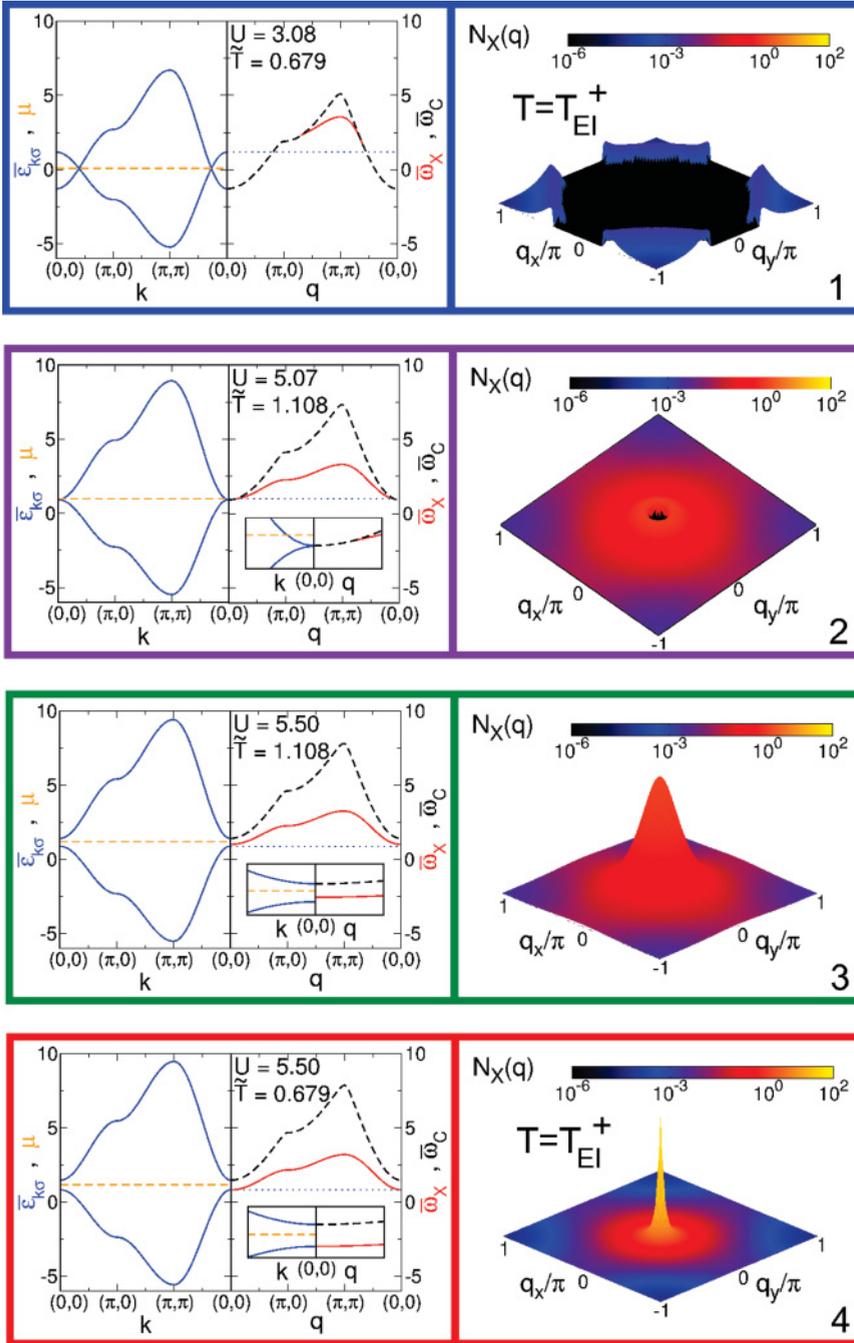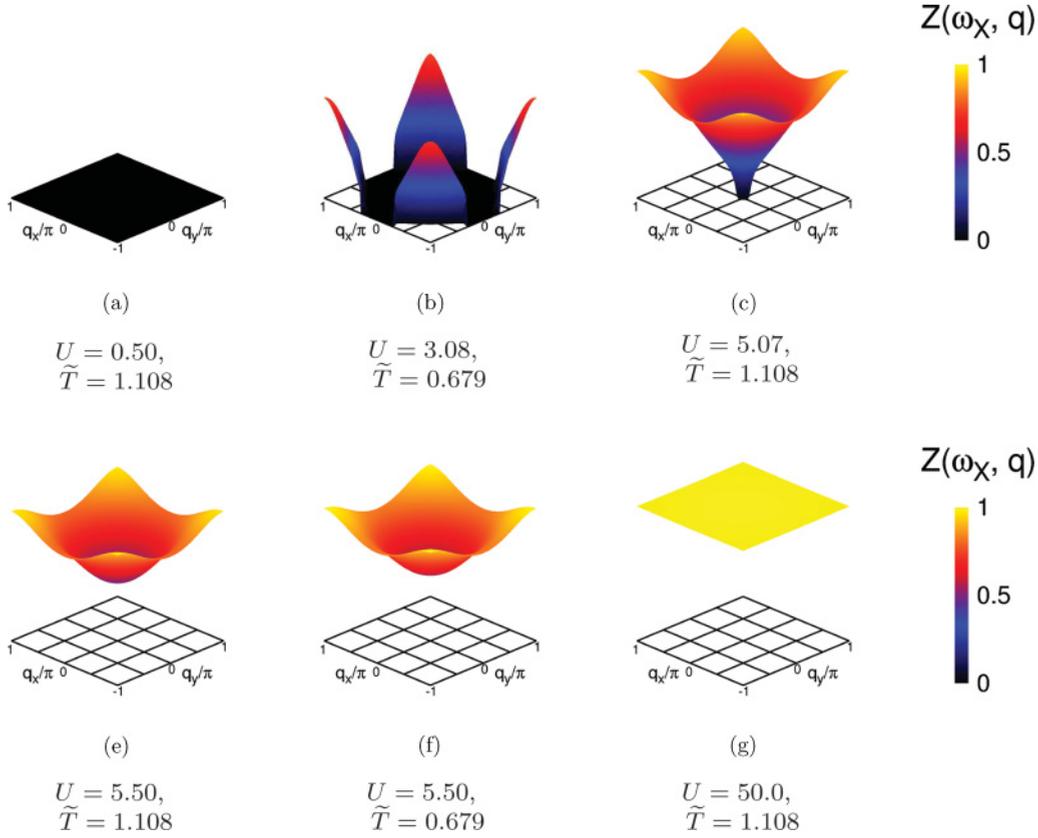
FIG. 2. (Color online) Mean-field band scheme (left-hand panels) and **q**-resolved exciton numbers (right-hand panels) for the points marked in Fig. 1 (1: at the SM-EI transition; 2: at the SM-SC transition; 3: in the SC regime; 4: at the SC-EI transition). The electron dispersion ($\bar{\varepsilon}_{\mathbf{k}\sigma}$) is given by the blue/dark gray solid lines, and the chemical potential (μ) by the orange/gray dashed line. Note that the excitonic level [$\omega_X(\mathbf{q})$, red/gray solid line] and the continuum level [$\omega_C(\mathbf{q})$, black dashed line] are shifted by the ↑-band maximum, $\bar{\omega}_{X/C} = \omega_{X/C} + \max_{\mathbf{k}}(\bar{\varepsilon}_{\mathbf{k}\uparrow})$. The blue/dark gray dotted line marks the ↑-band top.

band and finally touches its top at $\mathbf{k} = 0$ (point 4 in Fig. 1, red frame in Fig. 2). Thereby the excitonic instability appears, and the SC-EI transition takes place. Most notably, we observe a divergence of $N_X(0)$, i.e., the zero-momentum excitonic state is macroscopically occupied. This demonstrates the BEC of preformed excitons, contrary to the BCS-like transition on the SM side.

The spectral weight $Z(\omega_X,\mathbf{q})$ apparently accounts for the character and composite nature of the electron-hole bound states. This becomes especially evident in the weak and strong interaction limits. For very small U, the Coulomb attraction between electrons and holes can neither form excitonic bound states nor establish the c-f electron coherence in the EI state. Here $Z(\omega_X,\mathbf{q}) = 0$, independent of $\mathbf{q}$ [see Fig. 3(a)]. By

contrast, as $U \to \infty$, $Z(\omega_X,\mathbf{q}) = 1 \ \forall \mathbf{q}$ [Fig. 3(g)]. Hence, in this limit, excitons behave as ideal bosons; cf. Eq. (5). For $U \to \infty$, $\omega_X(\mathbf{q})$ scales as $\ln U$ while the continuum level grows $\propto U$ [recall that $\omega_C(0) = -E_\uparrow - 4(1 + |t_\uparrow|) + U(n_\uparrow - n_\downarrow)$]; E_B^X becomes infinite. Despite this, an EI phase cannot be established, this time because the large band splitting prevents c-f electron coherence. This explains why the EI phase arises below an upper critical coupling U_c only.

Having identified the nature and the condensation mechanism of electron-hole pairs we now discuss how they might influence the normal-state properties of the EFKM. In particular, we examine the so-called halo phase around the EI, where excitons and excitonic resonances dominate the electron-hole excitation spectrum.[2,17] Figure 4 gives results
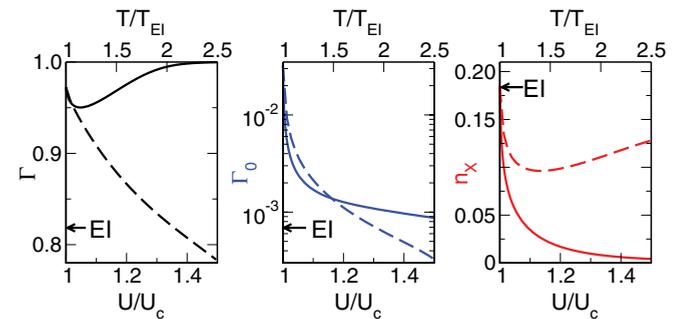
FIG. 3. (Color online) Exciton quasiparticle weight $Z(\omega_X, \mathbf{q})$.

for the SC region with $U > U_c(T)$ and $T > T_{EI}(U)$. Already for $U/U_c(T) \simeq 1.5$ almost all electron-hole pair excitations constitute excitons, i.e., $\Gamma \to 1$. The small number of nearly-free $\downarrow$ electrons can be attributed to the relatively large band gap. Remarkably, the portion of excitons with $\mathbf{q} = 0$ is less than one per thousand. Approaching U_c from above, by reducing U at fixed temperature, the fraction of the zero-momentum excitons increases by two orders of magnitude, thereby overcompensating the initial depletion of Γ caused by the reduction of U. Thus, on the SC side the formation of the EI is driven by the condensation of zero-momentum excitons. Keeping U constant and coming up to the EI by lowering the temperature, we observe an uninflected increase of both Γ and Γ_0 which again is triggered by the occupation of excitonic bound states with $\mathbf{q} = 0$. Here the initial decrease of n_X results from the narrowing of the Bose distribution. For temperatures of about $T/T_{EI}(U) \simeq 2.5$, we find a significant number of unbound $\downarrow$ electrons. Their contribution increases, if T is further raised, because excitons dissociate.

Figure 5 illustrates what happens if we cross the border to the SM phase at fixed $\tilde{T} > 1$ by reducing the bare band splitting $|E_\uparrow|$ (middle panel) or downsizing U (right-hand panels). On the SC side, n_X increases because the band gap decreases and concomitantly the exciton level deepen. In the SM, zero-momentum excitons cannot exist, and Γ_0 drops to zero. Although small, Γ is finite nevertheless, because electron-hole bound states carrying a finite momentum remain. These excitonic resonances will affect the transport properties on the SM side as well. Thus, basically the whole EI phase is

surrounded by an exciton-rich region (halo); there the number of charge carriers is substantially reduced, and excitons provide abundant scattering centers for the residual electrons and holes. We expect that an inclusion of the continuum electron-hole scattering states will round off the sharp kinks appearing in Fig. 5 at the SC-SM transition.[18]

Now we relate our results to experiments on the SC-SM transition in TmSe$_{0.45}$Te$_{0.55}$.[5–8] The anomaly in the lattice expansion as a function of temperature at high constant pressure occurring near 250 K was ascribed to a SM-EI transition, and the ratio of the exciton density n_{ex} and the

FIG. 4. (Color online) Bound-state fractions Γ and Γ_0 as functions of Coulomb attraction U at fixed $\tilde{T} = 0.679$ (solid lines, lower scales), and as functions of temperature at fixed $U = 5.5$ [dashed lines, upper scales; here T is given in units of $T_{EI}(U = 5.5)$]. The right-hand panel shows the corresponding exciton densities n_X.
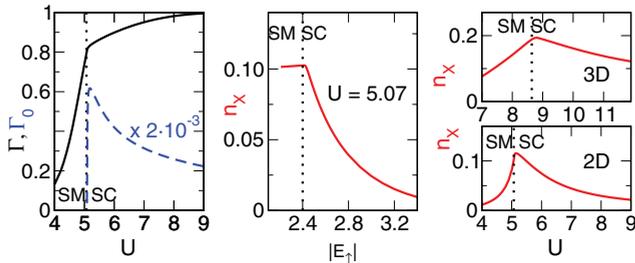
FIG. 5. (Color online) Bound-state fractions Γ (solid line) and Γ_0 (dashed line) as functions of the Coulomb attraction U (left-hand panel), and exciton density n_X vs bare band splitting $|E_\uparrow|$ (middle panel), both at $\widetilde{T} = 1.108$. The right-hand panels compare the U dependence of n_X for the 2D and 3D cases (at the same reduced temperature $\widetilde{T}$).

atomic density $n_{\rm Tm}$ was estimated as $n_{\rm ex}/n_{\rm Tm} = 0.22$ in Ref. 7. Assuming Mott-Wannier-type excitons, they are suggested to overlap due to their large concentration. However, the binding energy was found to be too large,[6] which questions the Mott-Wannier-type model. In our EFKM model, the coherence length $r_{\rm coh}$ of the excitons at $T = 0$ and for $U \sim 3.6$ equals the lattice constant (see Fig. 1 and Ref. 4). At the SC-EI transition at $T_{\rm EI}(U = 5.5)$ we obtain $n_X \sim 0.18$ (see Fig. 4, right-hand panel), and a BEC of nonoverlapping Frenkel-type excitons with a high density takes place. The numerical value of n_X at the SC side of the phase diagram approximately agrees with the experimental value [note that the agreement improves for the (real) 3D situation—see Fig. 5, upper-right-hand panel]. Taking the f bandwidth $W_\uparrow = 8|t_\uparrow| \simeq 30$ meV (Ref. 7) and

our parameter choice, we get $T_{\rm EI}^{\rm max} \simeq 0.3t_\downarrow \simeq 20$ K. That means, the experimental phase boundary at the SC side between 20 and 250 K obtained by electrical resisistivity data[5–8] describes the appearance of an exciton-rich halo phase above the SC-EI transition, as was also concluded in Ref. 2. On the other hand, the observed linear increase of the heat conductivity and thermal diffusivity with decreasing temperature below 20 K (Ref. 8) may be ascribed to the EI phase. As revealed by measurements of the Hall constant at 4.2 K as function of pressure,[5] the position of the maximum in the resistivity coincides with that of the minimum in the current-carrier density. We suggest that this close relation, indicating the formation of excitons from free current carriers, also holds in the halo phase. Then the maximum in n_X at the SC-SM transition (see Fig. 5) should correspond to a minimum in the current-carrier density, so that the resistivity maximum at the pressure-induced SC-SM transition in TmSe$_{0.45}$Te$_{0.55}$ may be qualitatively understood within our halo-phase concept.

In summary, we have analyzed the formation of the EI state at the SM-SC transition in the 2D EFKM and provided strong evidence for a BCS-BEC crossover scenario. While Cooper-type pairing fluctuations become critical on the SM side, Bose condensation of preformed zero-momentum excitons takes place on the SC side. Accordingly, the surroundings of the EI are dominated by electron-hole fluctuations or excitonic bound states with strong impact on the transport and optical properties.

[1] B. I. Halperin and T. M. Rice, Rev. Mod. Phys. **40**, 755 (1968).

[2] F. X. Bronold and H. Fehske, Phys. Rev. B **74**, 165107 (2006).

[3] D. Ihle, M. Pfafferott, E. Burovski, F. X. Bronold, and H. Fehske, Phys. Rev. B **78**, 193103 (2008).

[4] K. Seki, R. Eder, and Y. Ohta, Phys. Rev. B **84**, 245106 (2011).

[5] B. Bucher, P. Steiner, and P. Wachter, Phys. Rev. Lett. **67**, 2717 (1991).

[6] J. Neuenschwander and P. Wachter, Phys. Rev. B **41**, 12693 (1990).

[7] P. Wachter, Solid State Commun. **118**, 645 (2001).

[8] P. Wachter, B. Bucher, and J. Malar, Phys. Rev. B **69**, 094502 (2004).

[9] Y. Wakisaka, T. Sudayama, K. Takubo, T. Mizokawa, M. Arita, H. Namatame, M. Taniguchi, N. Katayama, M. Nohara, and H. Takagi, Phys. Rev. Lett. **103**, 026402 (2009); T. Kanaeko, T. Toriyama, Y. Ohta, and T. Konishi (unpublished).

[10] C. Monney, E. F. Schwier, M. G. Garnier, N. Mariotti, C. Didiot, H. Cercellier, J. Marcus, H. Berger, A. N. Titov, H. Beck, and P. Aebi, New J. Phys. **12**, 125019 (2010); C. Monney, C. Battaglia, H. Cercellier, P. Aebi, and H. Beck, Phys. Rev. Lett. **106**, 106404 (2011).

[11] Y. E. Lozovik and A. A. Sokolik, JETP Lett. **87**, 55 (2008); H. Min, R. Bistritzer, J.-J. Su, and A. H. MacDonald, Phys. Rev. B **78**, 121401 (2008); V.-N. Phan and H. Fehske, e-print arXiv:1202.0900.

[12] A. J. Leggett, in *Modern Trends in the Theory of Condensed Matter*, edited by A. Pekalski and R. Przystawa (Springer, Berlin, 1980); C. Comte and P. Nozières, J. Phys. (France) **43**, 1069 (1982); P. Nozières and S. Schmitt-Rink, J. Low Temp. Phys. **59**, 195 (1985).

[13] C. D. Batista, Phys. Rev. Lett. **89**, 166403 (2002); C. D. Batista, J. E. Gubernatis, J. Bonča, and H. Q. Lin, *ibid*. **92**, 187601 (2004).

[14] P. Farkašovský, Phys. Rev. B **77**, 155130 (2008); C. Schneider and G. Czycholl, Eur. Phys. J. B **64**, 43 (2008).

[15] B. Zenker, D. Ihle, F. X. Bronold, and H. Fehske, Phys. Rev. B **81**, 115122 (2010); **83**, 235123 (2011).

[16] N. M. Plakida, Springer Ser. Solid-State Sci. **171**, 173 (2011).

[17] V.-N. Phan, K. W. Becker, and H. Fehske, Europhys. Lett. **95**, 17006 (2011).

[18] G. Röpke, Ann. Phys. **3**, 145 (1994).